UDC 551.526.6:551.46.065:551.507.362.2:551.521.18

THE DETERMINATION OF SEA-SURFACE TEMPERATURE FROM SATELLITE HIGH RESOLUTION INFRARED WINDOW RADIATION MEASUREMENTS

W. L. SMITH, P. K. RAO, R. KOFFLER, and W. R. CURTIS
National Environmental Satellite Center, ESSA, Washington, D.C.

ABSTRACT

A statistical histogram method is developed to objectively determine sea-surface temperature from satellite high resolution window radiation measurements. The method involves inferring the distribution of surface radiances for the clear atmospheric case from observed histograms of generally cloud-contaminated radiances. The brightness temperature associated with the clear atmosphere modal peak radiance is the statistically most probable surface temperature. The reliability of the inferred surface temperature depends upon the number of cloud-free measurements available to define the clear mode. The method accounts for atmospheric attenuation and instrumental noise and also objectively discriminates cloud-free from cloud-contaminated observations.

The statistical histogram method is applied to 3.8 micrometer window radiation data obtained by the High Resolution Infrared Radiometer flown on the Nimbus 2 and Nimbus 3 satellites. Examples of sea temperatures inferred over both small and large areas are presented. Comparisons with conventional ship observations indicate that both bias and random errors of the inferred sea temperatures are less than 1°C.

Due to the apparent success of this statistical histogram technique, plans have been made to use it to obtain sea-surface temperatures on a global basis daily from operational high resolution infrared radiation measurements.

1. INTRODUCTION

Beginning in 1970, operational meteorological satellites will be carrying high resolution infrared radiometers. These radiometers are primarily useful to map nighttime cloud cover and to estimate cloud heights. Where there are no clouds in the field of view of the satellite, these "window" measurements effectively sense the temperature of the earth's surface. Thus, the advent of these infrared measurements operationally makes possible the routine preparation of global synoptic maps of sea-surface temperature. A number of papers (Curtis and Rao 1969, Greaves et al. 1968, Rao 1968, Rao et al. 1969, and Warnecke et al. 1967) have been published claiming that the horizontal sea-surface temperature distribution can be obtained from these infrared measurements. Most of them showed temperature distribution over very limited areas (particularly the Gulf Stream region) and never attempted to show the distribution over large areas.

Before any attempts can be made to process the data in terms of sea-surface temperature on an operational basis, an objective method of determining sea temperature from these data must be developed and tested. The objective of the present article is to formulate and test a simple and reliable statistical histogram technique for obtaining the global distribution of sea-surface temperature on a routine basis.

The radiation data used in this study were obtained by the 3.8-micrometer (μm) High Resolution Infared Radiometer (HRIR) instruments flown on the Nimbus 2 and Nimbus 3 satellites. A complete description of these instruments is given in the *Nimbus II User's Guide* and the *Nimbus III User's Guide* (U.S. Goddard Space Flight Center 1966, 1969). Only nighttime 3.8-μm HRIR data were considered for specifying sea temperature since the radiation measured in this spectral channel during the day is contaminated with reflected solar radiation. The techniques developed here are applicable to the 11-μm window measurements that will be made by the operational scanning radiometers.

The histogram technique formulated here is used to derive sea-surface temperature distributions over local as well as large oceanic domains. Where ship observations exist, they are used to verify the satellite-derived sea temperatures. It should be pointed out at the outset of this paper that differences between the two sea temperatures are not necessarily due to errors in either or both of the two measures. This is because the radiation window temperatures measured from satellites are most closely related to the surface "skin" temperature while sea-surface temperatures measured by standard techniques are usually the "subsurface" temperatures. Although the two measurements should not be radically different, significant differences can occur, depending on the wind condition.

As will be shown, the sea temperature inference method presented in this paper accounts for atmospheric water vapor and carbon dioxide attenuation, cloud contamination, and instrumental noise. These factors are certainly the most important to be considered for inferring sea temperatures from satellite window radiance measurements. Other factors such as bias due to errors in instrumental calibration, nonunity surface emissivity, and attenuation by minor atmospheric observing constituents were not specifically taken into account in deriving the

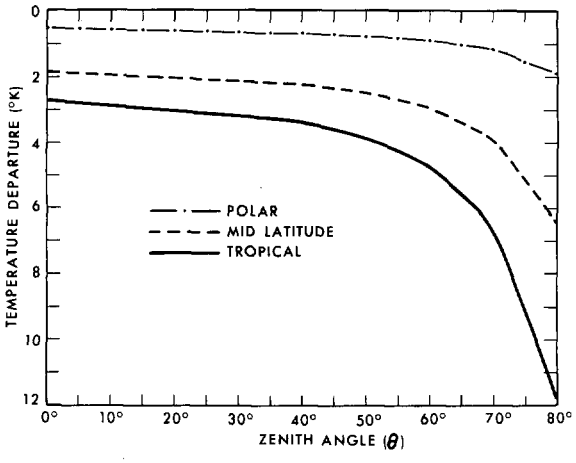

FIGURE 1.—Calculated departure of Nimbus HRIR temperature from ground surface temperature as a function of local zenith angle for three different airmasses.

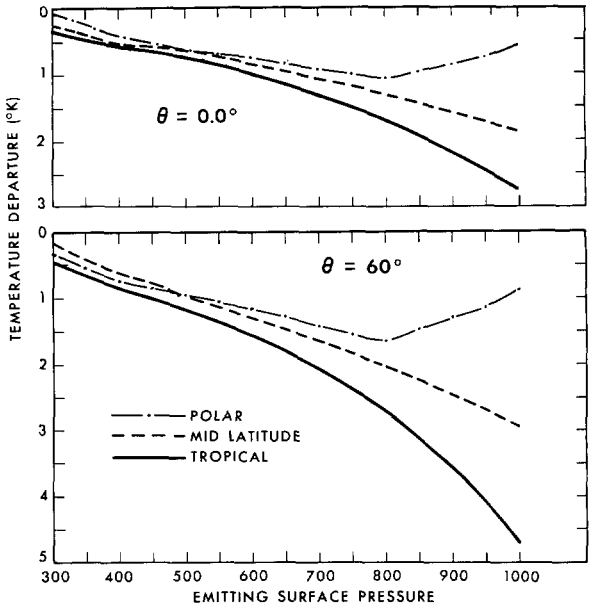

FIGURE 2.—Departure of Nimbus HRIR temperature from cloud temperature as a function of cloud pressure for two different zenith angles.

sea temperatures presented here. However, an empirical means of minimizing all sources of discrepancies between satellite and conventional observations of sea temperature is given.

2. METHOD OF INFERENCE

A. ATMOSPHERIC ATTENUATION CORRECTION MODEL

Before sea-surface temperature can be inferred from satellite HRIR window data, it is necessary to correct the measurements for any atmospheric contribution to the observed signal. In the 3.8-μm window region, atmospheric water vapor and carbon dioxide are the major absorbing constituents. The atmospheric contribution varies most significantly with the viewing angle of observation, cloud conditions, and the amount of precipitable water within the atmosphere.

Theoretical radiative transfer calculations were performed to determine the effect of atmospheric absorption and reemission on the outgoing radiation measured by the HRIR. The radiation leaving the earth's atmosphere and passing through the Nimbus 2, 3.8-μm filter was computed assuming model polar, midlatitude, and tropical temperature and water vapor profile conditions. The model atmospheres were chosen to reflect a representative range of surface temperature and total water vapor amount. Carbon dioxide was assumed to be uniformly mixed at 0.031 percent by volume in each atmosphere. Water vapor and carbon dioxide transmittances tabulated by Stull et al. (1964) and Wyatt et al. (1964) were used for the computations. Variations of outgoing radiation due to variations in viewing angle and cloud condition were determined.

Figure 1 shows for each model atmosphere the difference between surface temperature and the computed brightness (or equivalent blackbody) temperature as a function of the local zenith angle at the ground. For these calculations, the atmospheres were assumed to be cloud-free with a surface emissivity of unity. As may be seen for a given zenith angle, the temperature discrepancy increased with decreasing latitude due to increasing water vapor amounts. (The total precipitable water was 0.15, 1.2, and 4.7 cm for the polar, midlatitude, and tropical model atmospheres, respectively.) The temperature discrepancies increase at an increasing rate with local zenith angle, especially for "wet" atmospheric conditions. This feature is commonly referred to as "limb darkening." The limb-darkening curves shown in figure 1 indicate that absorption and reemission by atmospheric water vapor causes the largest discrepancy between surface temperature and 3.8-μm brightness temperatures observed under clear-sky conditions.

Figure 2 shows for two local zenith angles the discrepancy between satellite "observed" 3.8-μm brightness temperatures and the radiating temperature of an emitting cloud as a function of the pressure-altitude of the cloud. An interesting feature is the maximum departure at 800 mb in the polar atmosphere. This is caused by the low-level temperature inversion characteristic of the polar model atmosphere. The calculations shown in figure 2 also indicate that the atmosphere above the 400-mb level is nearly transparent to the radiation sensed by the 3.8-μm HRIR.

Figure 3 shows computed temperature departures (that is, departures of satellite-observed brightness temperatures from the cloud and ground surface radiating temperatures) as a function of satellite-observed brightness temperature. As may be seen, there is a high correlation between the

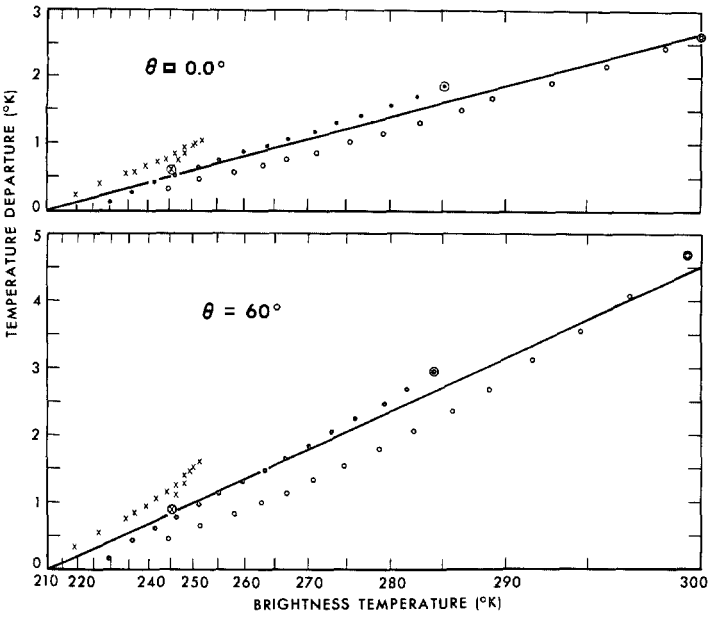

FIGURE 3.—Departure of Nimbus HRIR brightness temperature from ground and cloud radiating temperature as a function of "observed" brightness temperature. The crosses, dots, and open circles pertain to the polar, midlatitude, and tropical model atmospheres, respectively.

temperature departure produced by atmospheric absorption and the actual observed brightness temperature for a given viewing angle regardless of the emitting surface pressure. This is due to the fact that the water vapor and carbon dioxide attenuation is naturally correlated with the surface radiating temperature since it decreases with increasing cloud height and increasing latitude.

The above atmospheric characteristic makes it possible to predict the temperature discrepancy caused by atmospheric attenuation from the observed brightness temperature and the known viewing angle of measurement. This relationship has been found for local zenith angles of less than 60° to be expressible as

$$\Delta T=\left[a_0+a_1\left(\frac{\Theta}{60^\circ}\right)^{a_2}\right]\ln\left(\frac{100^\circ}{310^\circ-T_B}\right)$$

$$(210^\circ\text{K}\leq T_B\leq 300^\circ\text{K and } \Theta\leq 60^\circ)$$

where $a_0=1.13$, $a_1=0.82$, $a_2=2.48$, T_B is the observed brightness temperature in degrees absolute, and Θ is the local zenith angle of measurement. The corrections for brightness temperatures greater than 300°K or lower than 210°K can be assumed to be equal to those for 300°K and 210°K, respectively. It has been found that the correction for atmospheric attenuation cannot be predicted adequately for local zenith angles greater than 60°.

The temperature departure ΔT is added to the measured brightness temperature T_B to correct the observation for the contribution of the atmosphere above the viewed surface.

The values of the coefficients a_0, a_1, and a_2 given above and used in this paper were obtained from theoretical computations considering only H_2O and CO_2 as absorbing constitutents. It is noted, however, that these coefficients could be obtained empirically from an adequate statistical sample of actual satellite-observed clear-sky brightness temperatures and corresponding surface temperatures measured by conventional techniques. The empirically determined coefficients would account for the atmospheric attenuation by all absorbing constituents as well as account for any bias due to instrumental calibration error. New coefficients should be obtained for each new instrument, and even reevaluated periodically during the lifetime of a given instrument to account for degradation.

Although such empirical procedures seem optimum for the operational reduction of the data, they were not implemented for this study to maintain independence of satellite-derived surface temperatures from surface temperatures observed by conventional methods.

8. SEA-SURFACE TEMPERATURE DETERMINATION PROCEDURE

The mapping of sea-surface temperatures from satellite infrared window observations requires the ability to discriminate ground from cloud observations. With a single measurement, one might argue that the measurement is either of cloud or ground on the basis of the magnitude of the observed brightness temperature. Unfortunately, it is usually impossible to distinguish in this manner the difference between a relatively low opaque or even a high thin cloud from the surface since these temperatures may well be within 10°C of one another.

For overcoming this problem, it seemed promising to examine a relatively large number of measurements covering an area larger than that covered by clouds. From such a sample of measurements, one can determine the surface temperature making use of the facts that 1) the magnitude of the brightness temperature should be relatively high for clear observations and 2) the frequency of occurrence of a clear observation should also be high. The latter principal holds extremely well over the sea since the spatial variability of the sea-surface temperature is much smaller than the variability of the measured radiant temperatures produced by clouds.

The Nimbus HRIR scans contiguously from horizon to horizon in the direction perpendicular to the orbital track. The instantaneous ground resolution is about 4 n.mi. Frequency histograms of these high resolution measurements observed within given latitude/longitude areas were used to develop a technique for determining mean sea-surface temperature for the given area. In this study, 1.0°, 2.0°, and 2.5° latitude/longitude areas are considered. For 1° areas, more than 200 observations are generally available for specifying the sea-surface temperature; whereas for 2.5°, more than 1,000 observations are usually available.

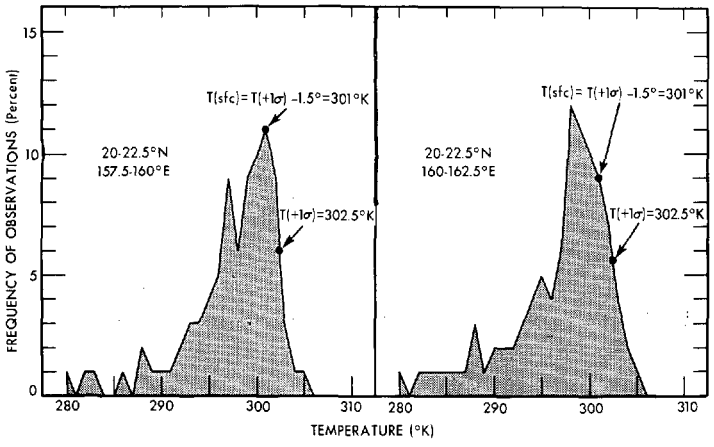

Figure 4.—Sample histograms of corrected Nimbus HRIR data showing their relation to sea-surface temperature.

In the absence of cloud-contaminated measurements, it is assumed that the distribution of satellite-observed temperatures is Gaussian with a dispersion produced by noise. Observed distributions in cases that appear to be cloud-free exhibit such a Gaussian character. The standard deviation, σ, of such distributions is equal to the known standard random error of measurement. For a Gaussian distribution, the temperature $+1\sigma$ from the mean or mode is that temperature on the high temperature wing of the distribution where the change of frequency of observation with temperature is a maximum. When a cloud-contaminated frequency distribution is obtained for an area, it is assumed that this maximum slope, or $+1\sigma$, point to the typical clear distribution (clear mode) is identifiable, provided there are sufficient clear spots within the area viewed. Thus, the surface temperature can be defined as the temperature at the point of maximum slope on the high temperature wing of the "clear mode" $T(+1\sigma)$, minus the standard error of measurement, σ. This value will usually be higher than the observed modal peak temperature when clouds exist, since in the cloudy case the observed brightness temperatures tend to be biased toward low temperatures.

For illustrating the technique, figure 4 shows two histograms of Nimbus 2 HRIR observations obtained over two adjacent 2.5° latitude/longitude areas. As may be seen, both distributions are skewed toward low temperatures due to cloud contamination. In fact, there were many values below 280°K which are not shown. The dispersion on the high temperature wing is mainly due to instrumental noise. The entire high temperature modes shown are produced by a combination of cloud-contaminated and cloud-free observations.

Assuming the high temperature wings of these modes near and beyond the $+1\sigma$ point are produced by cloud-free observations, the temperature at the $+1\sigma$ points of the clear modes can be determined. Since the standard error of measurements is about 1.5°K for the HRIR at these temperatures, the most probable surface temperatures are given by $T(+1\sigma)-1.5$°K.

Note that the inferred surface temperature for the more westerly grid square is the same as the modal peak temperature, indicating that the modal peak is produced predominantly by cloud-free observations. In the other area, however, the modal peak is 3°K lower than the inferred surface temperature, indicating that this peak is produced by cloud-contaminated as well as cloud-free observations. The observations greater than 301°K are apparently cloud-free, allowing the correct surface temperature to be inferred from the maximum slope of the distribution. The inferred temperatures are in agreement with a nearby ship observation of 301°K at 21° N., 156° E.

In specifying the sea-surface temperature from HRIR observations in this manner, additional precautions must be taken to insure that the high temperature wing of the "clear" mode is actually produced by cloud-free observations. High temperature wings produced by cloud-contaminated measurements can usually be discriminated from ones produced by cloud-free measurements since there is usually more dispersion in the cloud-contaminated wing. The greater dispersion is due to the increased variability of the observations produced by clouds. The only exception to this dispersion characteristic is the case where a low, thick, uniform overcast exists over the entire area of observation.

With such problems in mind, a complete set of procedures and precautions necessary for reliably specifying sea-surface temperatures from histograms of HRIR brightness temperatures, corrected for atmospheric attenuation, was devised. These are:

1) Determine whether a clear mode exists with the maximum frequency at a temperature greater than freezing (273°K). *Precaution:* If such a mode does not exist, too much cloud exists for specifying sea temperature.

2) Determine whether the maximum frequency of the clear mode is greater than 10 percent of the total number of observations. *Precaution:* If the maximum frequency is less than 10 percent, too much cloud exists for specifying the sea temperature.

3) Specify $T(+1\sigma)$ as the temperature where the change of frequency with brightness temperature on the high temperature wing of the clear mode is a maximum. *Precaution:* If the change of frequency with temperature is less 3 percent (deg K)$^{-1}$, the wing of the clear mode is considered to be influenced by cloud-contaminated measurements and consequently the surface temperature cannot be specified.

4) Specify the surface temperature as the difference between $T(+1\sigma)$ and the standard error measurement. *Precaution:* If the difference between the specified temperature and the highest observed brightness temperature, with the frequency of observation greater than 1 percent, is greater than 3σ (for example, 4.5°K for $\sigma=1.5$°K), then the wing of the clear mode is considered to be in-

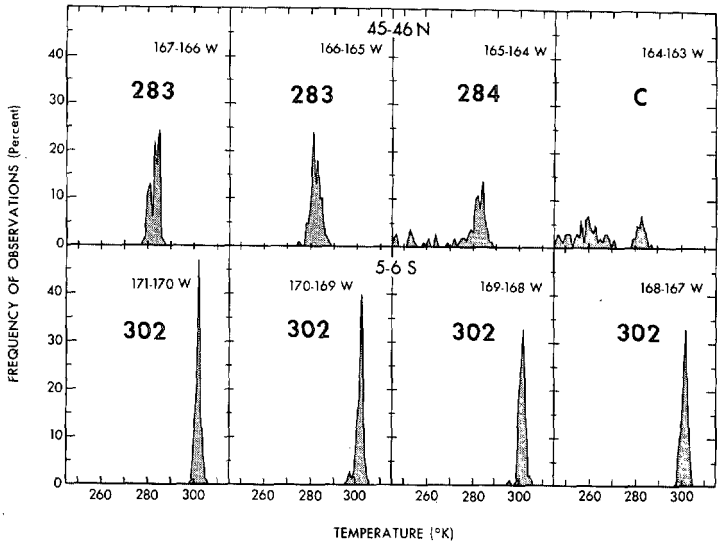

FIGURE 5.—Sample histograms of Nimbus 2 HRIR data on Oct. 8, 1966. The derived temperatures (°K) are given. C denotes an indeterminate temperature due to excessive cloudiness.

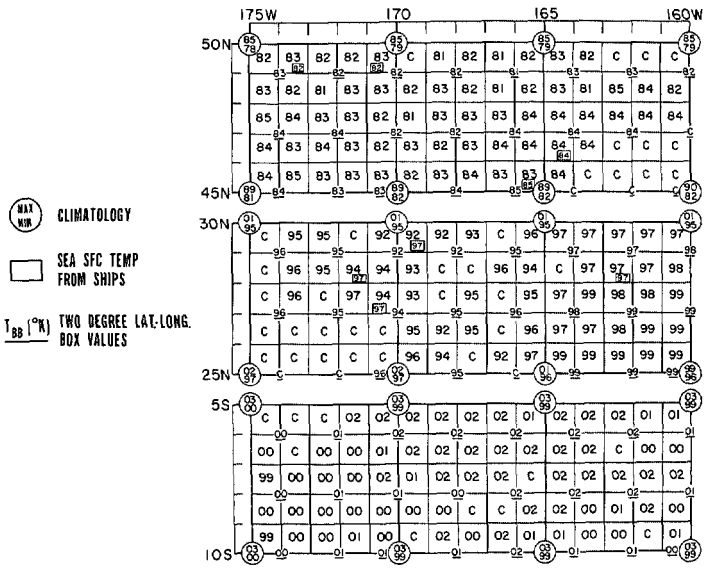

FIGURE 6.—Surface temperature derived from 1° histograms of Nimbus 2 HRIR data obtained on Oct. 8, 1966. Temperatures are in degrees Kelvin with the first digit deleted. (Add 300 to values <10; add 200 to values >10.)

fluenced by cloud-contaminated measurements and consequently the surface temperature cannot be specified.

Figure 5 shows some typical histograms, together with inferred surface temperatures, for 1° latitude/longitude areas. These examples reveal the stability of the histogram technique on the 1° area scale. The stability, of course, increases with area size or through time compositing since the number of observations that are available for defining the clear modal distribution increases.

The procedure given above for specifying sea-surface temperature is completely objective. As such, it can be implemented by digital computer, thus enabling bulk processing of satellite HRIR data. Sea temperatures for areas where severe cloud contamination exists, or which are not observed due to gaps in satellite data coverage, can be inferred through space and time interpolation procedures.

3. RESULTS

For localized studies of the sea-surface distribution a 1° latitude/longitude histogram grid size appears optimum. With this grid resolution, there are usually enough observations to define the clear mode, and subsequently the sea-surface temperature adequately, while still maintaining fairly high geographical resolution. A larger grid size (for example, 2.0° or 2.5°) is preferable for large-scale hemispheric or global analyses.

Figure 6 shows an example of surface temperatures derived over the mid-Pacific from 1° and 2° histograms of Nimbus 2 HRIR data. The temperatures derived for each grid square are printed. The C's denote areas where sea temperatures could not be derived on the basis of the precautions given in the procedure outlined above. This example shows that the derived temperatures are generally very stable, especially on the 2° grid scale, and agree within reasonable limits with available ship reports and climatology. The only exception to the remarkable agreement noted above is in the 25°–30° N./165°–172° W. area. Here, the derived sea temperatures appear to be about 2°–5°K too low. It can be seen from the histograms (not shown) and from the relatively large number of C's that this area possesses very substantial amounts of cloudiness. It is obvious that, at least in a few cases, the histogram technique failed to differentiate completely between cloud-free and cloud-contaminated brightness temperatures. This failure is probably due to the existence of a low-level overcast that radiatively and statistically "appears" to be clear.

Erroneous sea temperatures, like the ones noted above, could be filtered out of the analysis using reasonable spatial gradient consistency checks and/or through time compositing. Such techniques should eliminate erroneous estimates since correct surface temperatures are usually derived, even in relatively cloudy areas. Evidence of this is given by the 297°K temperature derived for the 27°–28° N./171°–172° W. region which is in good agreement with two nearby ship observations.

Figure 7 shows sea-surface temperatures derived over the Caribbean from Nimbus 3 nighttime HRIR observations. This is the period when the BOMEX (Barbados Oceanographic Meteorological Experiment) was in progress. Sea-surface temperatures obtained from five BOMEX ships are also shown. In spite of a relatively high degree of broken cloudiness over the region, there is relatively good agreement between the satellite-derived temperatures and the ship-reported temperatures. As expected, the sea

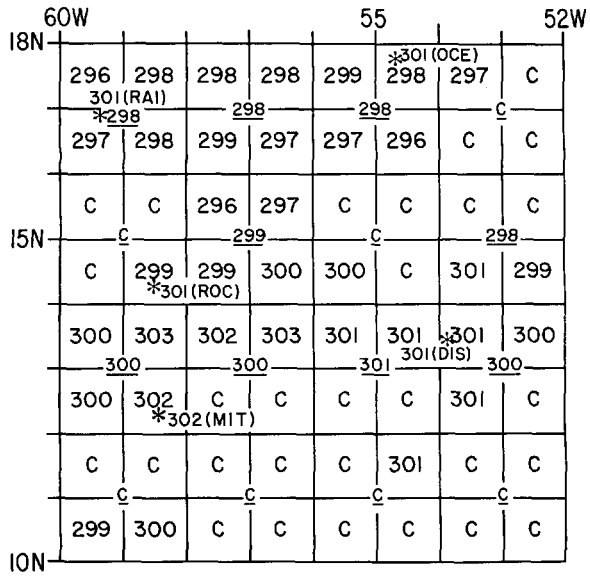

FIGURE 7.—Surface temperatures (°K) derived from Nimbus 3 HRIR (nighttime) data Orbit 681 on June 4, 1969. The values shown in the center of each box were derived from 1° histograms while the underlined values were derived from 2° histograms. The asterisks are BOMEX ship observations. C denotes indeterminate temperatures due to excessive cloudiness.

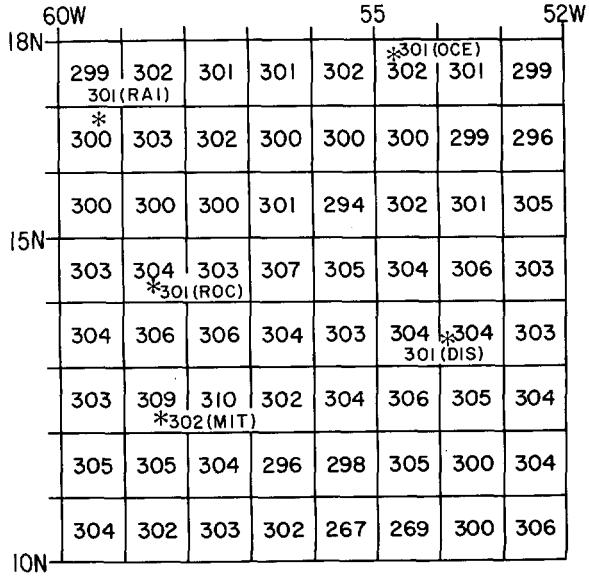

FIGURE 8.—Highest brightness temperatures in each latitude/longitude box from Nimbus 3 HRIR (nighttime), Orbit 681 on June 4, 1969.

temperatures derived from 2° histograms appear to be less noisy than those derived from the 1° histograms.

One might ask whether the highest brightness temperature observed within a grid area can be used as an estimate of the sea-surface temperature. The reasoning behind this question is that the highest brightness temperature has the greatest probability of not being affected by any clouds.

Figure 8 shows the highest brightness temperatures observed within the 1° grid areas illustrated in the previous figure. The highest values range from 267°K to 310°K. The 267°K is obviously a cloud-contaminated measurement while the 310°K temperature was probably caused by instrumental noise. As may be seen, the highest temperatures are extremely spatially unstable due to cloud and instrument noise. As a result, they do not provide any useful information on the true sea-surface temperature distribution. A comparison of figures 7 and 8 illustrates the effectiveness of the histogram technique in suppressing the effects of clouds and instrumental noise in specifying the sea-surface temperature.

It has been mentioned earlier that data gaps due to cloudiness might be overcome through time compositing. Before deciding on the required number of days for compositing, one should examine the data coverage gained by adding a day at a time. Even though clouds associated with a certain synoptic system generally dissipate or move out of a region, other clouds associated with another synoptic system might develop or move into the region. By compositing a day at a time, one can approximately determine the number of days required to get the maximum coverage. Unbiased compositing is, of course, based on the assumption that the sea-surface temperature over the area has not changed significantly during the period under consideration. This assumption is probably quite valid for relatively short periods. Biasing will be minimized by deriving the temperature for each unit area from the composite frequency distributions. This method properly weights each day's observations with respect to the existing cloud conditions.

Figure 9 shows, for an initially cloudy portion of the Pacific Ocean, how the surface temperature coverage increased through daily 1° histogram compositing. After 3 days, surface temperatures were obtained for all but a very small area of persistent cloudiness. On the 2.5° grid scale, there were no data gaps over this region after 3 days of compositing.

Figure 10 shows the surface temperature distribution of the Pacific Ocean obtained from 3-day composite 2.5° histograms of Nimbus 2 nighttime HRIR data. The isotherms are drawn at a 2°K interval. The large-scale features of this analysis agree well with climatology. For example, the cold California Current about 35° N. and the warm Alaska Current north of 40° N. off the west coast of the United States are quite apparent in the derived analysis. The coastline of Australia is also delineated quite well, the interior of Australia at night being generally colder than the surrounding sea.

Finally, figure 11 shows a scatter diagram of sea-surface temperatures derived for the North Pacific from HRIR data compared with those reported by ships. The RMS difference is about 1.7°K. However, there is a bias difference of 1°K so that the relative discrepancies are general-

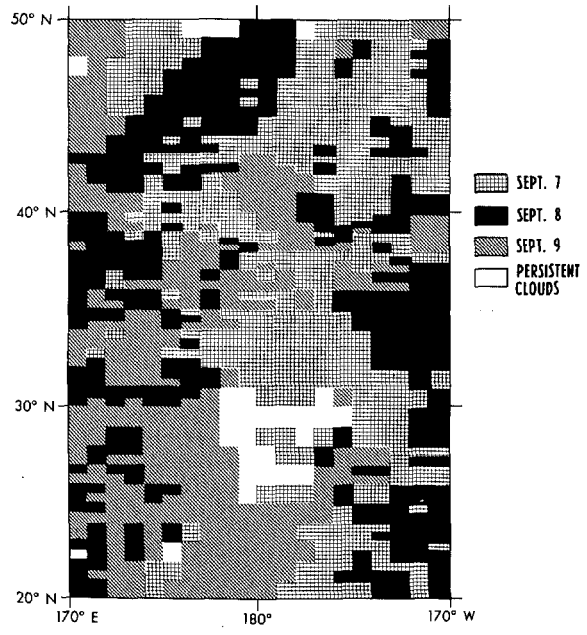

FIGURE 9.—Surface-temperature coverage obtained by daily compositing of Nimbus 2 HRIR data.

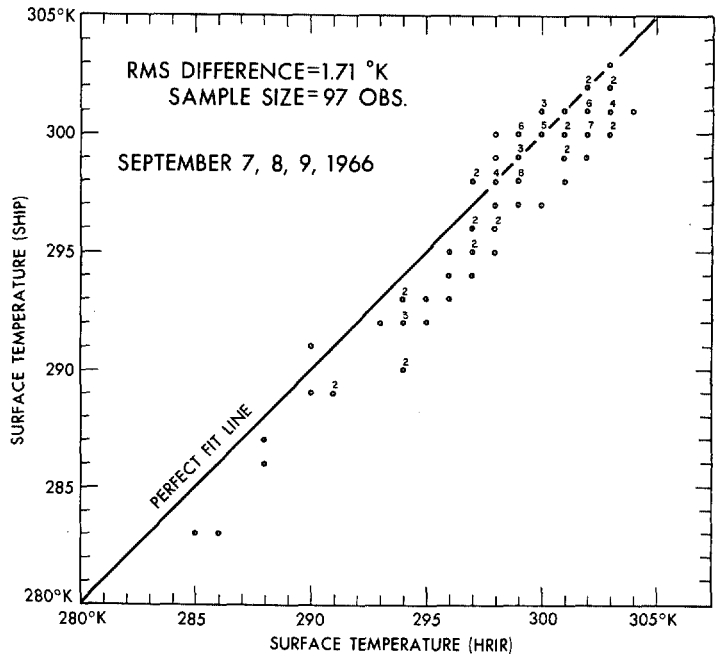

FIGURE 11.—Scatter diagram of surface temperatures obtained from ships and inferred from Nimbus 2 HRIR data.

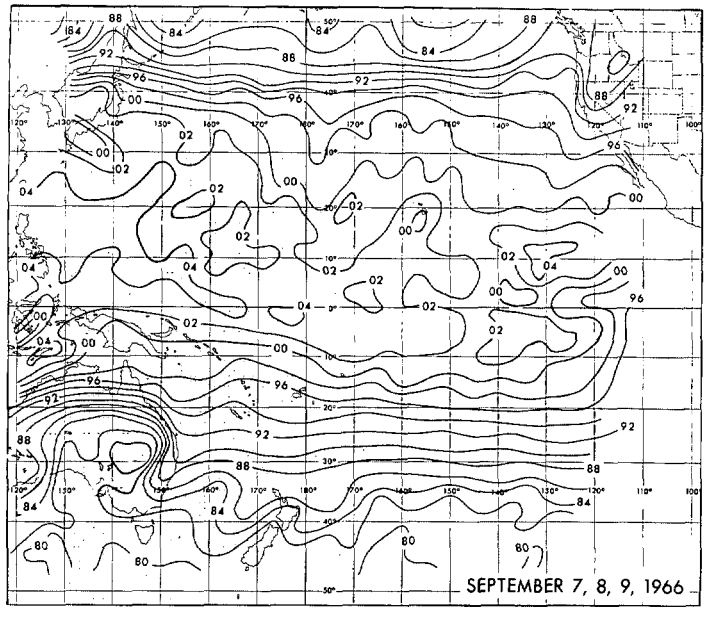

FIGURE 10.—Three-day composite Pacific Ocean surface-temperature analysis inferred from Nimbus 2 HRIR data. Isotherms are labeled in degrees Kelvin with the first digit deleted. (Add 300 to values <10; add 200 to values >10.)

ly less than 1°K. The bias difference could be due to a real difference between "skin" and subsurface temperature as measured by ships or may be caused by the instrumental calibration of the HRIR. The bias discrepancies could be alleviated by the empirical calibration technique outlined at the end of subsection 2A. The fact that the relative discrepancies are generally less than 1°K seems quite significant in view of the probable errors of the ship reports.

4. SUMMARY AND FURTHER COMMENTS

A technique for deriving sea-surface temperatures has been developed and tested with a limited amount of data. The technique is purely objective and minimizes the influence of atmospheric absorption, cloud contamination, and instrumental noise on the inferred sea temperatures. The verification results presented here indicate that a relative accuracy of better than 1°K can be achieved, especially with the aid of time compositing and/or objective spatial analysis of the data. A technique has also been presented (subsection 2A) for calibrating the absolute values of satellite-observed brightness temperatures with sea temperatures observed by conventional techniques.

Due to success of the objective statistical histogram method of inferring sea temperature, global analyses of sea temperature can be derived on an operational basis using future satellite data. Such operational analyses are currently planned to be initiated in the summer of 1970.

ACKNOWLEDGMENTS

In any study of this nature that involves a vast amount of data, particularly from satellites, team effort is necessary and especially for programming and analysis. We would like to thank Warren Jacob, Paul Pellegrino, Simon Roman, and Julia Hart for helping us with the data analysis and Leonard Hatton for drafting the figures. Finally our thanks to Messrs. G. Cherrix and L. Allison of the NASA Goddard Space Flight Center for providing the Nimbus 2 and Nimbus 3 HRIR data.

REFERENCES

Curtis, William R., and Rao, P. Krishna, "Gulf Stream Thermal Gradients From Satellite, Ship, and Aircraft Observations," *Journal of Geophysical Research, Oceans and Atmospheres*, Vol. 74, No. 28, Dec. 20, **1969**, pp. 6984–6990.

Greaves, J.R., Willard, J. H., and Chang, D. T., "Observations of Sea Surface Temperature Patterns and Their Synoptic Changes Through Optimal Processing of Nimbus 2 Data," *Final Report*, NASA Contract NAS W–1651, Allied Research Associates, Concord, Mass., Sept. **1968**, 121 pp.

Rao, P. K., "Sea Surface Temperature Measurements From Satellites," *Mariners Weather Log*, Vol. 12, No. 5, Sept. **1968**, pp. 152–154.

Rao, P. K., Curtis, W. R., Strong, A. E., and McClain, E. P., "Remote Sensing of Sea Surface Temperature," *Proceedings of the Sixth Space Congress, Cocoa Beach, Florida, March 17–19, 1969*, Canaveral Council of Technical Societies, Cape Canaveral, Fla., **1969**, 10 pp.

Stull, V. Robert, Wyatt, Philip J., Plass, Gilbert N., "The Infrared Transmittance of Carbon Dioxide," *Applied Optics*, Vol. 3, No. 2, Feb. **1964**, pp. 243–254.

U.S. Goddard Space Flight Center, NASA, *Nimbus II User's Guide*, National Aeronautics and Space Administration, Greenbelt, Md., July **1966**, 229 pp.

U.S. Goddard Space Flight Center, NASA, *Nimbus III User's Guide*, National Aeronautics and Space Administration, Greenbelt, Md., **1969**, 238 pp.

Warnecke, Guenther, Allison, Lewis J., and Foschee, Lonnie L., "Observations of Sea Surface Temperatures and Ocean Currents From Nimbus II," *NASA Report* No. X–622–67–435, National Aeronautics and Space Administration, Goddard Space Flight Center, Greenbelt, Md., **1967**, 9 pp.

Wyatt, Philip J., Stull, V. Robert, and Plass, Gilbert N., "The Infrared Transmittance of Water Vapor," *Applied Optics*, Vol. 3, No. 2, Feb. **1964**, pp. 229–241.

[*Received April 23, 1970*]